Monthly Progress Report ARCHES PR-11 & PR-12

on

Antennas in Reconfigurable High-Impedance Electromagnetic Surfaces

covering the period

1 August 2000 to 30 September 2000

submitted to

John Turtle
Air Force Research Laboratory
Antenna Technology Branch
AFRL/SNHA
31 Grenier St.
Hanscom AFB, MA 01731-3010
John.Turtle@hanscom.af.mil

Prepared by

Victor Sanchez
Senior Engineer
Titan Systems Corporation – Atlantic Aerospace Division
6404 Ivy Lane, Suite 300
Greenbelt, MD 20770
(301) 982-5271
sanchez@titan.com

Under Contract Number F19628-99-C-0080

26 October 2000

1.0 Cost Summary

The actual expenses for the fiscal month of August 2000 were $108,625, and the cumulative actual expenses for the entire program through the end of August 2000 are 644,313. The actual expenses for the fiscal month of September 2000 were $90,078, so that the cumulative actual expenses for the entire program through the end of September 2000 are $732,160. Through September we continued to under-spend relative to the original plan. However, we anticipate a significant increase in program activity in the October/November timeframe. The total contract funding level is currently $1,531,000.

2.0 Man Hours Expended

The man-hours expended for the August/September reporting periods were 392 and 387 respectively. The cumulative man-hours expended are 3520 and 3907 respectively. Shown below in Figure 1 is a summary of labor hours by labor grade, along with cost per labor grade for the month reported. Engineer 3 is the lowest paid labor grade working on this program, with program manager being the highest labor grade and a most of the work being performed by an Engineer 5.

TITAN SYSTEMS CORPORATION
ATLANTIC AEROSPACE DIVISION

ARCHES - BAA 99-19
August 2000 1555

	Current Month		Cumulative	
DIRECT LABOR	**Hours**	**Cost**	**Hours**	**Cost**
Engineer 3	198	22,609	1,789	208,514
Engineer 4			262	33,458
Engineer 5	184	31,523	1,267	223,665
Engineer 6			10	1,941
Program Manager/Engineer	10	2,073	193	48,175
	392	**56,206**	**3,520**	**515,753**

	Current Month	Cumulative
ODCs with Material Handling Fee	**Cost**	**Cost**
Materials	19,278	31,877
No Fee Subcontractor	32,875	81,086
Subcontractors		
	52,153	**112,963**

	Current Month	Cumulative
OTHER DIRECT COSTS	**Cost**	**Cost**
In-house Cosultants		
Miscellaneous	0	2,524
Rental Materials		
Travel	266	13,073
	266	**15,598**

TOTAL PROGRAM COST	**108,625**	**644,313**
Committments		24,129
TOTAL PROGRAM COST + Committments		**668,442**
Budget At Completion		**2,500,564**

Figure 1a. Summary of the August costs by labor grade and ODCs.

TITAN SYSTEMS CORPORATION
ATLANTIC AEROSPACE DIVISION

ARCHES - BAA 99-19
September 2000 1555

DIRECT LABOR	Current Month Hours	Current Month Cost	Cumulative Hours	Cumulative Cost
Engineer 3	221	24,319	2,010	232,069
Engineer 4			262	33,109
Engineer 5	166	29,137	1,433	251,854
Engineer 6			10	1,941
Program Manager/Engineer			193	47,941
	387	**53,456**	**3,907**	**566,913**

ODCs with Material Handling Fee	Current Month Cost	Cumulative Cost
Materials	19,157	50,909
No Fee Subcontractor	13,156	94,460
Subcontractors		
	32,313	**145,369**

OTHER DIRECT COSTS	Current Month Cost	Cumulative Cost
Cosultants	4,019	4,019
In-house Cosultants		
Miscellaneous	290	2,810
Rental Materials		
Travel		13,049
	4,309	**19,878**

TOTAL PROGRAM COST	**90,078**	**732,160**
Committments		21,255
TOTAL PROGRAM COST + Committments		**753,415**
Budget At Completion		**2,500,564**

Figure 1b. Summary of the September costs by labor grade and ODCs.

3.0 Schedule Status

During these two reporting periods, August & September 2000, the following tasks where pursued: Task 1.1 – Passive Broadband AMC Development, Task 1.2 – Reconfigurable Bandgap AMC Development, Task 2.1 – Identification of Desired Equivalent Media, Task 3.1 – Octave Array Demonstration, and Task 4.0 – Program Management. Refer Figure 2 below for the program schedule.

WBS	Task Name	Budget	Spent
0	ARCHES	$2,500,564	$644,313
1	Integrated Ground PlaneTechnical Dev.	$1,381,843	$416,041
1.1	Passive Broadband AMC Dev.	$325,981	$300,792
1.2	Reconfigurable Bandgap AMC Dev.	$545,363	$115,249
1.3	Switchable Element Development	$397,444	$0
1.4	Electronic Controls Development	$113,055	$0
2	Computational Tool Development	$604,994	$112,088
2.1	Identification of Desired Equiv. Media Prop.	$78,686	$64,462
2.2	Fast Solver Development	$41,650	$32,508
2.3	Realizability of the Desired Effective Medium	$131,605	$6,973
2.4	Spectral Domain Code Development	$252,408	$0
2.5	ASU Reports and Meetings	$57,311	$8,145
2.6	Transition Plan to Commercial Software	$43,334	$0
3	Array Demonstration	$286,774	$5,574
3.1	Octave(.2-2 GHz) Lab Demo	$286,774	$5,574
3.2	Decade (.2-2 GHz) Lab Demo	$0	
4	Meetings and Reports	$226,953	$110,611
4.1	TIMs	$93,243	$84,271
4.2	Monthly Status Reports	$37,755	$25,852
4.3	Annual Technical Reports	$95,955	$0

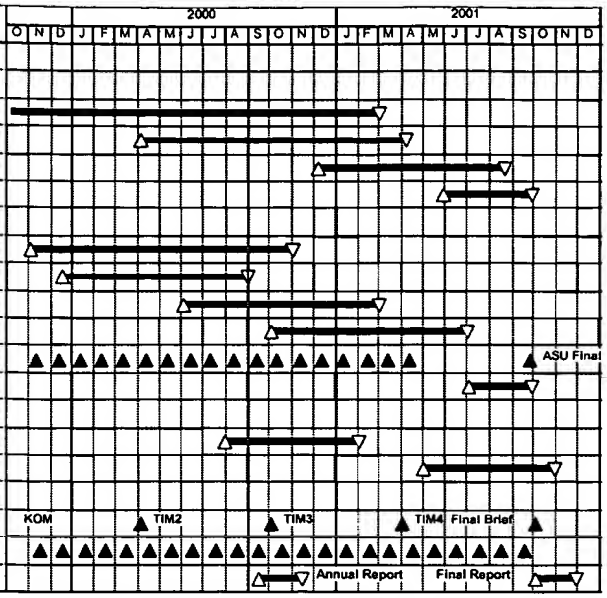

Figure 2a. ARCHES program schedule, budgeted costs, and spending through August 2000.

WBS	Task Name	Budget	Spent
0	ARCHES	$2,500,564	$732,160
1	Integrated Ground PlaneTechnical Dev.	$1,381,843	$452,828
1.1	Passive Broadband AMC Dev.	$325,981	$325,241
1.2	Reconfigurable Bandgap AMC Dev.	$545,363	$127,587
1.3	Switchable Element Development	$397,444	$0
1.4	Electronic Controls Development	$113,055	$0
2	Computational Tool Development	$604,994	$123,504
2.1	Identification of Desired Equiv. Media Prop	$78,686	$64,462
2.2	Fast Solver Development	$41,650	$36,151
2.3	Realizability of the Desired Effective Medium	$131,605	$14,691
2.4	Spectral Domain Code Development	$252,408	$18
2.5	ASU Reports and Meetings	$57,311	$8,183
2.6	Transition Plan to Commercial Software	$43,334	$0
3	Array Demonstration	$286,774	$40,835
3.1	Octave(.2-2 GHz) Lab Demo	$286,774	$40,835
3.2	Decade (.2-2 GHz) Lab Demo	$0	
4	Meetings and Reports	$226,953	$114,992
4.1	TIMs	$93,243	$88,330
4.2	Monthly Status Reports	$37,755	$26,174
4.3	Annual Technical Reports	$95,955	$0

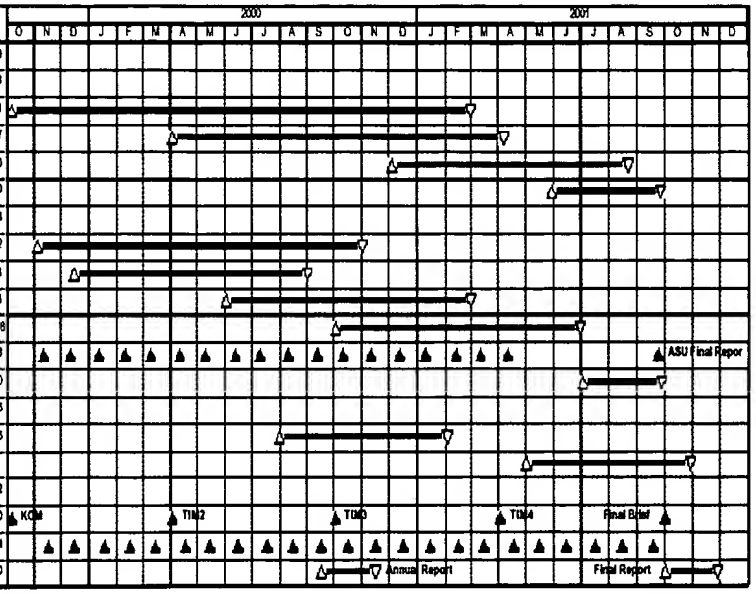

Figure 2b. ARCHES program schedule, budgeted costs, and spending through September 2000.

A breakdown of planned budget for each task is given in Figure 2 for each line item. The second column on this chart shows the cumulative amount spent per line item.

The burn curve through September is shown below in Figure 3. It shows we are underspending the plan. Both Atlantic Aerospace and ASU continue to spend below the original projected levels. However, we anticipate a significant increase in program activity in the October/November timeframe.

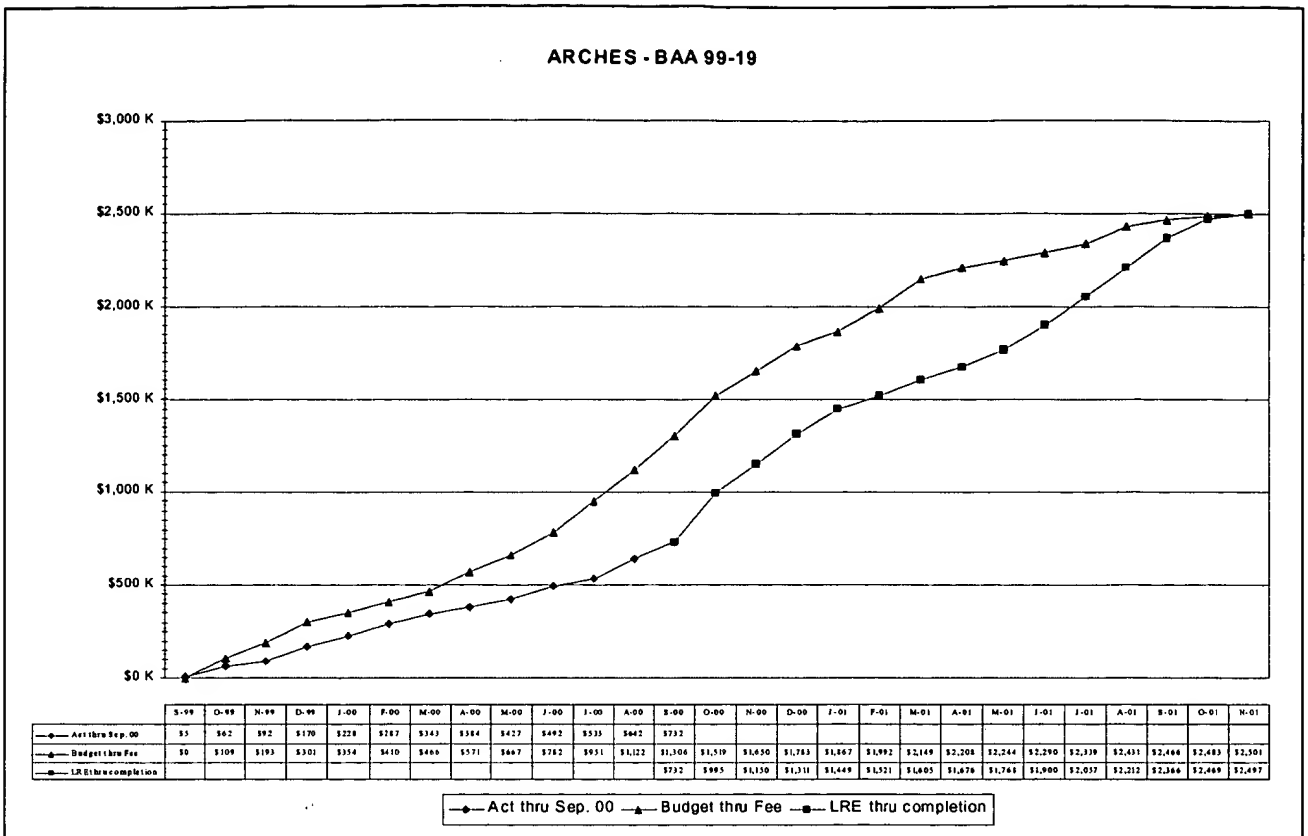

Figure 3. September 2000 Burn curves: actuals (blue), budget (red) and LRE through completion (magenta).

4.0 Technical Progress

Task 1.1 Passive Broadband AMC Development: The goal of this task is to design and demonstrate a passive AMC whose surface wave bandgap and impedance bandwidth is an octave in bandwidth for a structure whose electrical thickness is $\lambda_o/50$ at its resonant frequency ($f_o = c/\lambda_o$). In order to achieve this performance, we have determined that materials with permeabilities (μ') of about 5 and permittivities (ε') around 10 with low loss up to 2 GHz are necessary. Note: the derivation of these requirements is contained in the six-month technical interchange meeting, TIM-2, delivered April 10th, 2000.

As reported in TIM-2 and in the previous monthly status report, we have implemented a multi-threaded approach towards achieving these material requirements. The status of our various approaches is summarized below:

- **Unaligned Barium-Cobalt Hexaferrite Tile approach:**

Barium-Cobalt Hexaferrite - $Ba_3Co_2Fe_{24}O_{41}$ (also known in short hand as Co_2Z) has been demonstrated previously (Smit and Wijn, Ferrites, 1959, John Wiley & Sons). This approach is therefore deemed relatively low risk and is our baseline approach.

Tom Countis of Countis Labs had manufactured and tested several samples of this material. As described in the last status report, during the process, he discovered that repeating the results of Smit & Wijn is non-trivial. In addition to knowing the ingredients (*i.e.* $Ba_3Co_2Fe_{24}O_{41}$) the exact process of calcining, dry compaction and sintering is critical to obtaining high densities and the proper solid state reaction (*i.e.* crystal lattice). This process, which involves up to 2000 psi and a temperature profile reaching 1300° C over the course of one week, was not recorded in detail by previous authors.

In mid-August, we directed Countis Labs to use the remainder of our original contract monies to attempt further iterations on realizing a workable Co_2Z material – a "shotgun" approach using slightly different initial mixtures (impurities, etc.) and slightly different processing techniques. Note: these monies had originally been set aside to fabricate a large number of Co_2Z tiles as a substrate for our demonstration. Near the end of August, we brought Mr. Leo Brissette on board with a small consulting contract. Leo is retired, and had been the director of the microwave hexaferrite group at EMS, Technologies in Atlanta over the last 10 years or so. Leo had several substantive telecons with all of the other materials subcontractors to the ARCHES contract – including Tom Countis. Some of Leo's recommendations were incorporated into the various batches of ferrites being made in Tom's current experiment. The results of the experiment will be known in the late-October timeframe.

- **Barium-Cobalt Hexaferrite Powder in Elastomeric Binder approach:**

This approach is a risk/cost reduction alternative to the solid Co_2Z tiles. Arun Ranade of Particle Technologies is one of two vendors producing this powder. The results of the first vendor (Praxair) were not encouraging (reported upon in the last monthly status report).

During this reporting period, Particle Technologies did produce a small quantity of powder for testing at R&F products. However, because Particle Technologies is also working on the higher-priority iron-particle approach (described in the next section), no significant progress was made with regards to Co_2Z powder.

- **HQ-Iron Powder in Elastomeric Binder approach:**

This approach represents yet another alternative to the solid Co_2Z tiles. The approach is to use spherical iron particles suspended regularly in an elastomeric binder material. The particles investigated thus far are BASF's CIP and HQ grade iron powders. Both materials are composed of approximately 99% iron. The CIP particles, however, are up to 8 microns in diameter, whereas the HQ grade powder has a spectrum of particles no larger than 2 microns. With similar loading densities, both particles should produce similar artificial material properties, that is, the real parts of the permittivity and permeability for the two materials should be about the same. However, experiments (and

heuristic arguments regarding eddy currents) have shown that the HQ material has a lower magnetic loss factor than the CIP at frequencies of interest to us. The value of the loss using the HQ material makes it marginally useful for our application, however if we could reduce the losses slightly further, the resulting material could be very useful. The mechanism to achieve this would be to use smaller iron particles with similar (by weight) loading of the binder.

BASF was approached regarding smaller size particles. Their response was that they have not investigated smaller than 2 micron particles in the past because (a) nobody has expressed a desire for such particles and (b) smaller particles become pyrophoretic. That is, they have a tendency to spontaneously react with oxygen because their surface area is large relative to their mass. BASF also indicated that they are very busy producing their current products and are not interested in pursuing development of smaller particles at this time.

Our approach to achieving smaller particles was therefore to enlist our subcontractor, Dr. Arun Ranade of Particle Technologies to do particle classification and passivation. His approach was to disperse the particles in a liquid and use gravitational sedimentation to separate out the particle sizes (i.e. the larger, heavier particles will settle to the bottom of the liquid more quickly than the smaller particles, enabling him to separate them). Both the sizes of the particles in question and the composition (iron) have made this process problematic. Specifically, the particles seem to be "clumping" together due to magnetic and possibly electrostatic forces. Various additives (surfactants) have been used in order to separate the particles. Particle Technologies continues to experiment along these lines as well as with the possibility of using ultrasonic agitation to help separate the particles.

Once the particles are classified, we anticipate passivation using some insulating material (nominally silicon-dioxide) to reduce the pyrophoricity of the material. Following this, we will again impregnate an elastomeric binder, this time with particles that are 0.5 micron or lower, in an attempt to obtain as low-loss an artificial magnetic substrate as is possible.

Task 1.2 Reconfigurable Bandgap AMC Development: The purpose of this task is to analyze a reconfigurable AMC structure. The initial tuning mechanism to be investigated consists of varactor diodes placed across the patches of a single-layer the capacitive FSS to obtain variable capacitance, hence a variable tuning state for the AMC. This portion of this task was completed during the reporting period, and led to the demonstration of a reconfigurable AMC demonstration – discussed in task 3.1 below. The focus during this reporting period was on the varactor tuning method. However, there are other approaches to obtaining reconfigurable bandgaps (including pin diodes and other methods which tune the actual AMC substrate). We plan to investigate some of these methods in upcoming months.

- Analysis of a varactor tunable AMC. Part I: Reflection coefficient behavior

Consider an FSS consisting of an array of square plates where the unit cell is the highlighted 3x3 array in Figure 4.

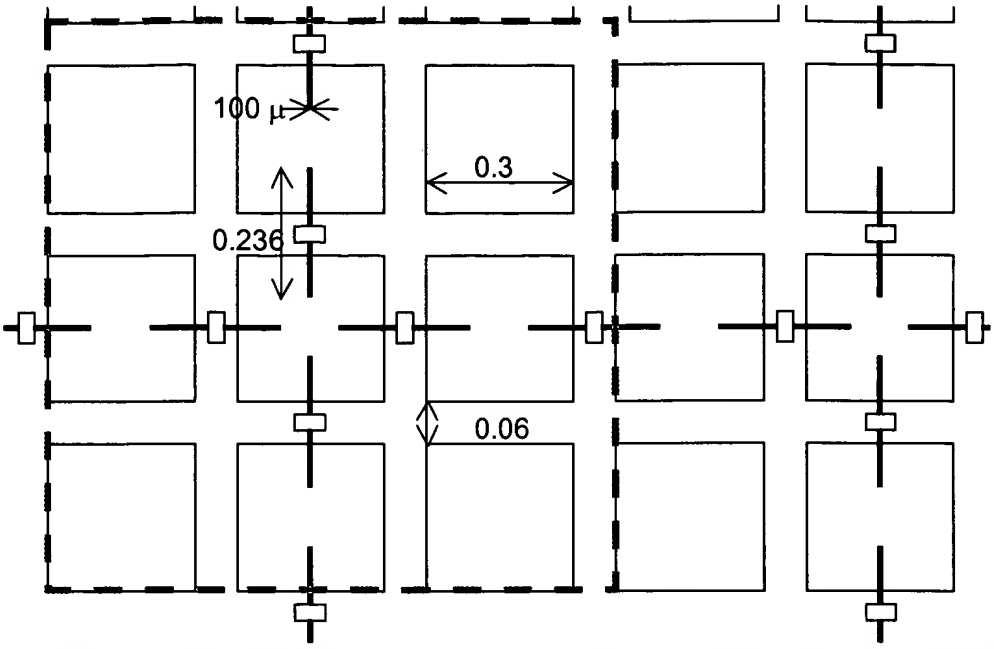

Figure 4. FSS array of squares in which a 3x3 unit cell is connected through varactors.

From the unit cell we can draw the equivalent circuit of Figure 5 and its simplification in Figure 6. Figure 6 also includes the values of the circuit elements.

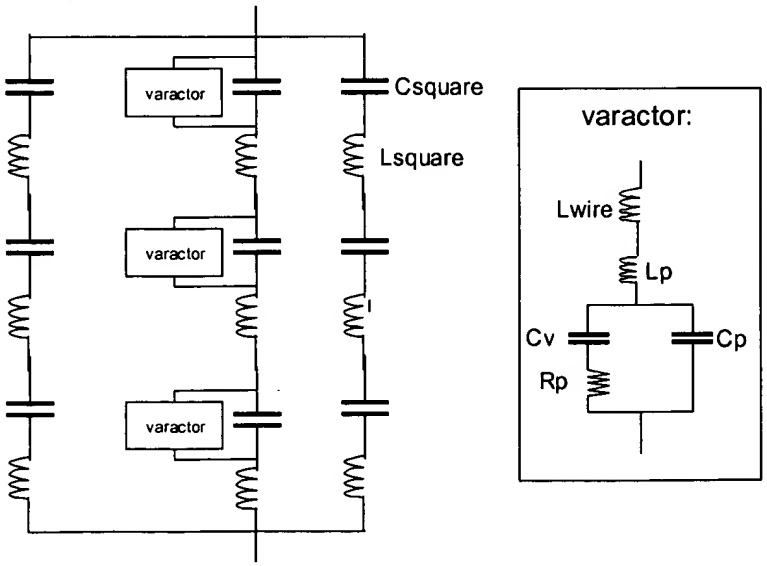

Figure 5. Equivalent circuit of the unit cell of Figure 1.

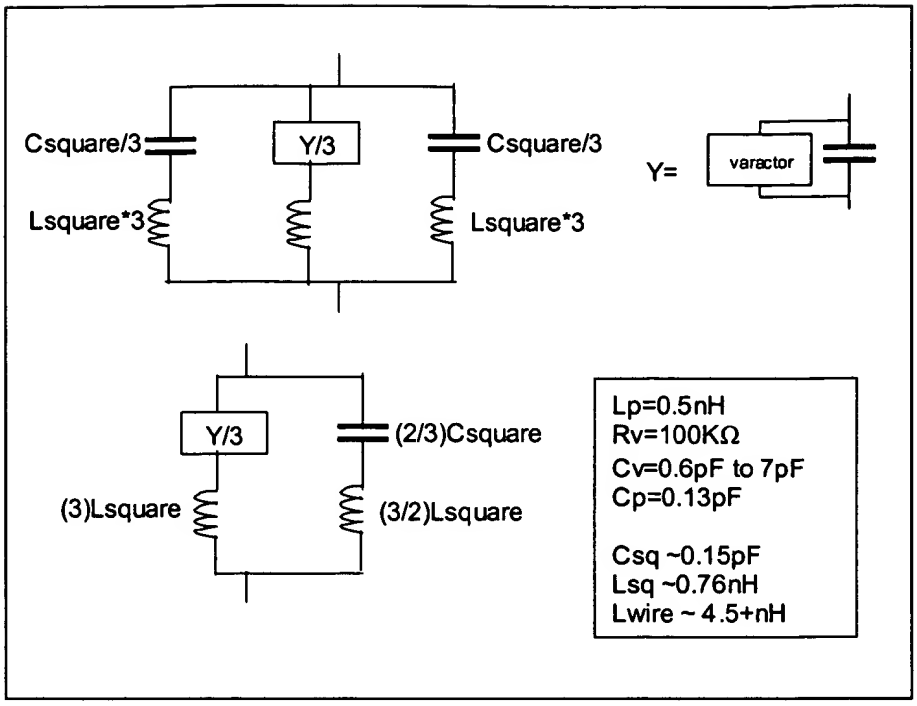

Figure 6. Simplification of the unit cell circuit and the values of the elements.

The varactor circuit element parameters were obtained from the manufacturer's data (M/A-COM MA46H202). The circuit parameters of the FSS are derived as follows.

The capacitance of the squares is taken to be approximately equal to that of an array of capacitive strips. Since the dielectric support (ε=3.38) of the squares is as thick as the edge-to-edge gap, we use an average permittivity for this capacitance of (1+3.38)/2. According to Marcuvitz Section 5.18, for an array of periodic unit p and gap g in free space, the normalized susceptance of the shunt obstacle on the free space transmission line is:

$$\frac{B}{Y_0} = \frac{4p}{\lambda} \ln\left(\csc\frac{\pi g}{2p}\right) \qquad (1.2.1)$$

This result is for normal incidence and ignores higher order terms that are small when g<p. Therefore,

$$C_{sq} = \frac{B}{377\omega}\left(\frac{1+3.38}{2}\right) = 0.1512pF \qquad (1.2.2)$$

Note that the approximation of complete capacitive strips is justified for the squares because the electric field in the side-to-side gap between squares is nearly zero, and charge accumulates at the corners of the squares thus approximately compensating for the "missing" area. (A more accurate result can be obtained by using Seymour Cohn's classic paper on the subject of square arrays.) On the other hand for the inductance, we expect the approximation of infinitely long strips to be coarser because the interruption of current flow by the gaps distorts the otherwise uniform current distribution.

Nevertheless, a reasonable approximation is to use the infinite strips result and to scale it by the actual length of the square in the unit cell.

According to Marcuvitz 5-19, the normal incidence reactance is:

$$\frac{X}{Z_0} = \frac{p}{\lambda}\ln\left(\csc\frac{\pi w}{2p}\right) \qquad (1.2.3)$$

where w is the width of the strips. Thus for our case:

$$L_{sq} = \mu_0 \frac{p}{2\pi}\ln\left(\csc\frac{\pi w}{2p}\right)\left(\frac{w}{p}\right) = 0.053nH \qquad (1.2.4)$$

The inductance of the squares is very low, suggesting that the square array will resonate around,

$$f_{sq} = \frac{1}{2\pi\sqrt{L_{sq}C_{sq}}} = 56.3GHz \qquad (1.2.5)$$

At such a high frequency the model for the inductance would be invalid, but the point to be made is that this frequency is much higher than the frequency at which we would expect an isolated square to resonate in the antenna mode because the inductance of a periodic array with small gaps is much lower than that of an isolated square, whereas the capacitance is not greatly increased by the edge-to-edge coupling.

We can use the same equation to obtain the inductance of the varactor leads as modeled in Microstripes. For a thin wire of radius r much smaller than p and length l, equation 1.2.4 becomes:

$$L_{wire} = \mu_0 \frac{p}{2\pi}\ln\left(\frac{p}{2\pi r}\right)\left(\frac{l}{p}\right) = 4.04nH \qquad (1.2.6)$$

Since we have ignored the segment of wire connecting the leads to the squares, I have estimated the total inductance of this portion of the circuit to be of the order of 4.5nH. BUT this is not the end of the story! Because the model in Microstripes has the wire 236 mils long, it must run above the metal squares for 176 mils of that length. We know that PECs in proximity to a tangential magnetic field, serve to concentrate (double) that magnetic field. Therefore, the length of wire running above the squares actually has more inductance than that estimated here. Another way of arguing this is to say that the presence of the wire concentrates the current flow on the squares and increases their self inductance. In either case, the series inductance of the square-lead combination must be of the order of 5nH **or greater**. (You could also expect some increase in the capacitance of the squares since before the varactor is placed at the ends of the leads, the leads bring the charges on the squares closer to each other, albeit with a very small plate area (100m diameter of the wire). However, I expect such a capacitance increase to be small.) Figure 7 illustrates all these phenomena.

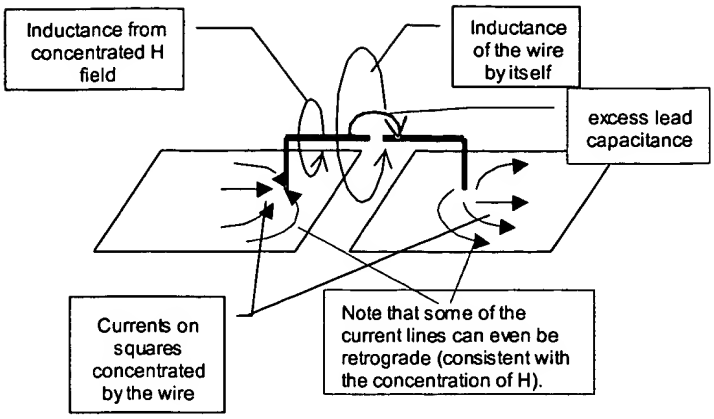

Figure 7. The connection of lead wires to the FSS squares dramatically alters the near fields responsible for the admittance of the FSS layer, even before the varactor is added.

These speculations could be confirmed by a Microstripes run in which the varactor or capacitor is not connected to the leads. What I have done is to take the 0.6pF pure capacitor Microstripes results that gave a center frequency of 1.705 GHz and bandedges at 1.548 and 1.784 GHz respectively, and added Capacitance to Csquare and Inductance to Lwire in my model until I got the same answer.

NOTE that in actual practice, the leads would most likely be completely soldered to the squares up to the edge. In that case, the length l is at most 0.06 inches, giving L_{wire} (minimum) = 1.03nH. (Plus the current concentration contribution on the squares).

Now to calculate the reflection coefficient of the AMC: The short, rolled through the lowest substrate of thickness t has an admittance:

$$Y_{short} = \frac{1}{i\eta_0 \sqrt{\frac{\mu_y}{\varepsilon_x}} \tan\left(k_0 t \sqrt{\mu_y \varepsilon_x}\right)}$$

Then we roll this admittance through the thickness of the FSS substrate to get the input admittance:

$$Y_{in} = Y_{top}\left(\frac{Y_{short}\cos\beta d + iY_{top}\sin\beta d}{Y_{top}\cos\beta d + iY_{short}\sin\beta d}\right)$$

where Y_{top} is the admittance of the FSS substrate $= \sqrt{3.38}/\eta_0$, d is the 60 mil thickness of the substrate, and β is $k_0\sqrt{3.38}$. The reflection coefficient then follows as usual. The result is that to match the pure 0.6pF capacitor result, I find that C_{square} is not changed by the leads significantly but there is an additional inductance added to L_{wire} and L_{square} of the order of 5.5nH, for a total excess series inductance in the circuit of 10nH *all due to the leads used to connect the varactor to the squares.*

Figure 8a, shows the resultant phase of the reflection coefficient for 0.6pF pure capacitor, while 8b shows it for a 7pF pure capacitor. The resonance of the former is around 1.7GHz and the latter around 0.53GHz.

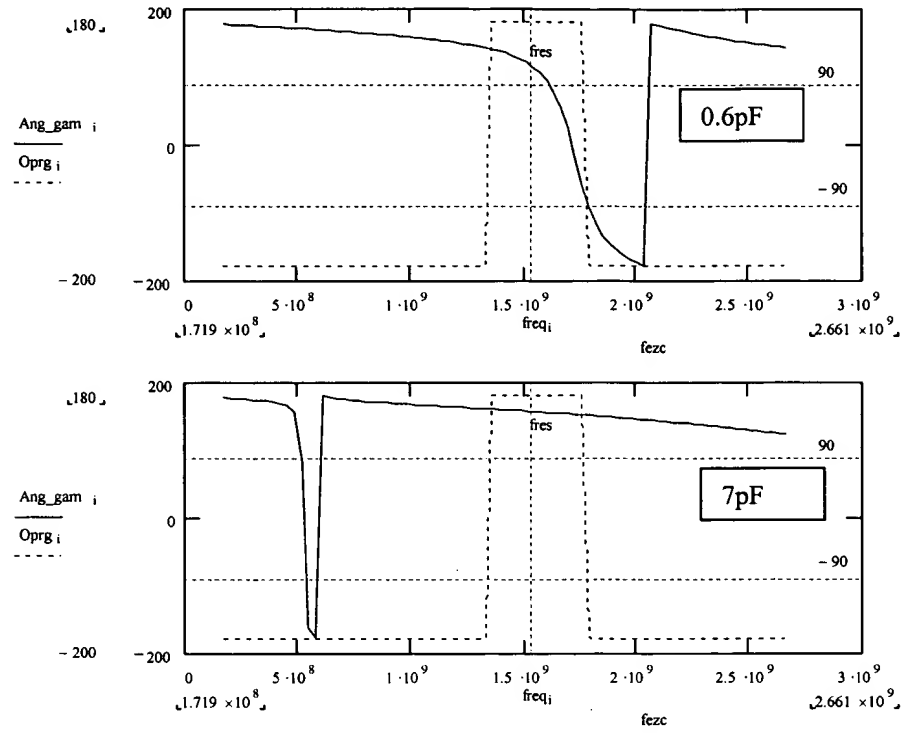

Then the results with varactors follow directly and these are shown in Figure 9. The resonances are now around 1.54 GHz and 0.5GHz respectively

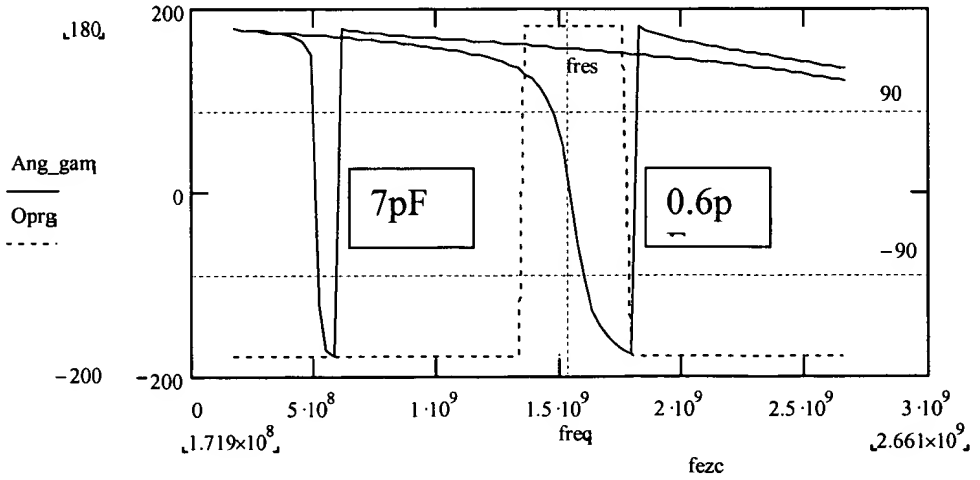

Figure 9. MathCad model of the 3x3 varactor tuned AMC including all parasitic inductances.

With this agreement with the Microstripes model we can explore what will happen under other circumstance. For instance, soldering the leads down over the whole length will drop the wire inductance to 1nH plus some residual current concentration effect. Let's assume a total of 2nH instead of 10nH. Then we get Figure 10, with the resonance tuning happening from 2.1GHz at 0.6pF to 0.77GHz at 7pF.

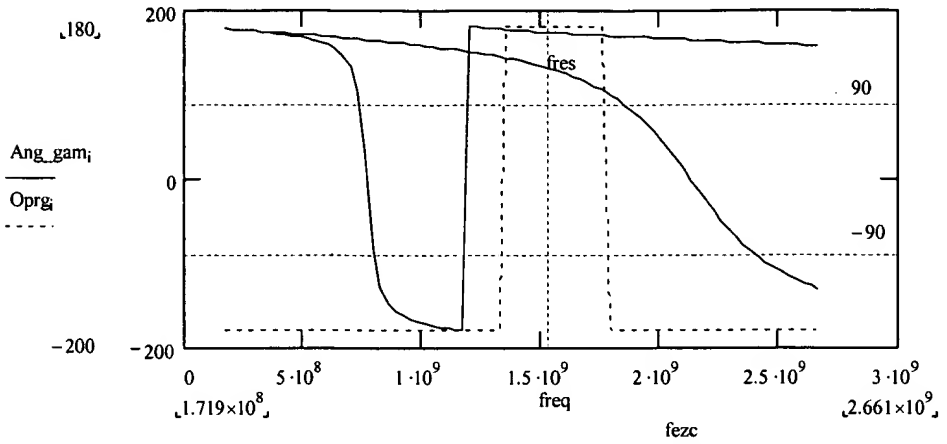

Figure 10. MathCad simulation of the result of completely soldering the leads of the varactor to the FSS squares in the 3x3 AMC design.

To obtain a top frequency of 1.7GHz, the FSS squares must have a much smaller gap (which will also reduce the lead inductance – but not necessarily the current concentration inductance). Even with a gap of 6mils the square capacitance only goes up to 0.4pF, leading to a top frequency of the order of 1.84GHz (assuming the excess lead inductance has dropped to 1nH). This is probably the smallest practical gap in a single layer design leading to a bottom frequency at 7pF of 0.82GHz. (see Figure 11).

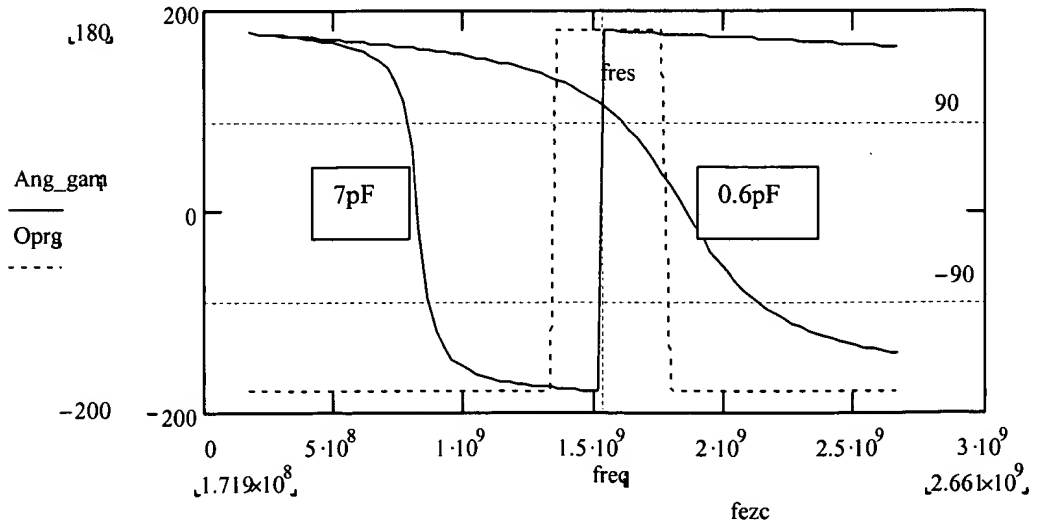

Figure 11. The 3x3 AMC design with FSS squares with only 6 mil gaps.

- Reflection Coefficient Behavior Conclusions:

With the present 3x3 design the selected varactors give a resonant frequency tunability range of 3:1, that is from 1.54 GHz to 0.511 GHz, with associated operational bandwidths of 11.3% and 3.08% respectively. If the squares are made bigger (so that the gap is 6 mils) and the leads shortened we can get a tunability range of 2.24:1, that is from 1.84GHz to 0.82GHz, with associated bandwidths of the order of 27% and 11% respectively.

Using an overlapping (two-layer) FSS capacitor layer, and minimizing the lead inductance (again assumed at 1nH), I estimate that a 0.73pF squares capacitance would lead to a tuning range from 1.55GHz to 0.79GHz (1.96:1) with operational bandwidths of 25% and 11% respectively.

The lesson is that series inductance added to the FSS can increase the tunability of varactor tuned AMCs by bringing down in frequency the LC resonance of the FSS layer. This causes a frequency dependent increase in apparent capacitance over the operational band that allows us to get lower frequency resonances but at the same time narrows the operational bandwidth. For narrow band requirements this could be a useful trick if we can accurately control all parasitic inductances.

- Analysis of a varactor tunable AMC. Part II: Surface wave behavior:

So as not to encumber the Surface Wave program with an additional dielectric layer, we absorb the 60mil FSS substrate into the squares' capacitance and make the bottom substrate thickness 300 mils (effective). The result for the 3x3 configuration is almost identical with that of Figure 9.

Now the critical issue is the TE mode suppression over the band of frequencies above the resonance, since this is affected by how low we can make the z-directed permittivity of the FSS. By definition a Cohn square FSS has $\mu_z \sim 2./\varepsilon_{geo}$, where ε_{geo} is the effective transverse permittivity of the FSS strictly due to the geometry (that is, ignoring the dielectric enhancement). For FSS with overlapping square this is alittle higher, $\mu_z \sim 2.4/\varepsilon_{geo}$. Thus since such FSS lead to AMCs with TE suppression, even when the FSS has an average substrate permittivity $\varepsilon_{avg} \sim (1+3.38)/2=2.2$, we can say that as long as the product $\mu_z \varepsilon_t \leq 5.3 = 2.2*2.4$we will have TE suppression.

Therefore in the case of varactor-tuned FSS we can expect a problem, because ε_{geo} is left unchanged (and therefore so is μ_z) but ε_t is increase above and beyond the contribution of the substrate by the added varactors. Indeed this is what happens for the 3x3 design. For this case the resonance in the MathCAD model occurs around 1.54 GHz, with the following reflection phase angles to either side: 1.5299 GHz is +26.8°, and at 1.5545 GHz

it is –18°. Whereas the upper band edge is around 1.59 GHz with the following angles to either side: 1.579 GHz is –63.7°, and at 1.604 GHz it is –99°
If there was surface wave suppression we would get no intersections between kx(Transverse Resonance) and the kx line until the neighborhood of 1.58GHz. Instead, as soon in Figure 12, as soon as we cross into negative angles (1.5545GHz) we get an intersection.

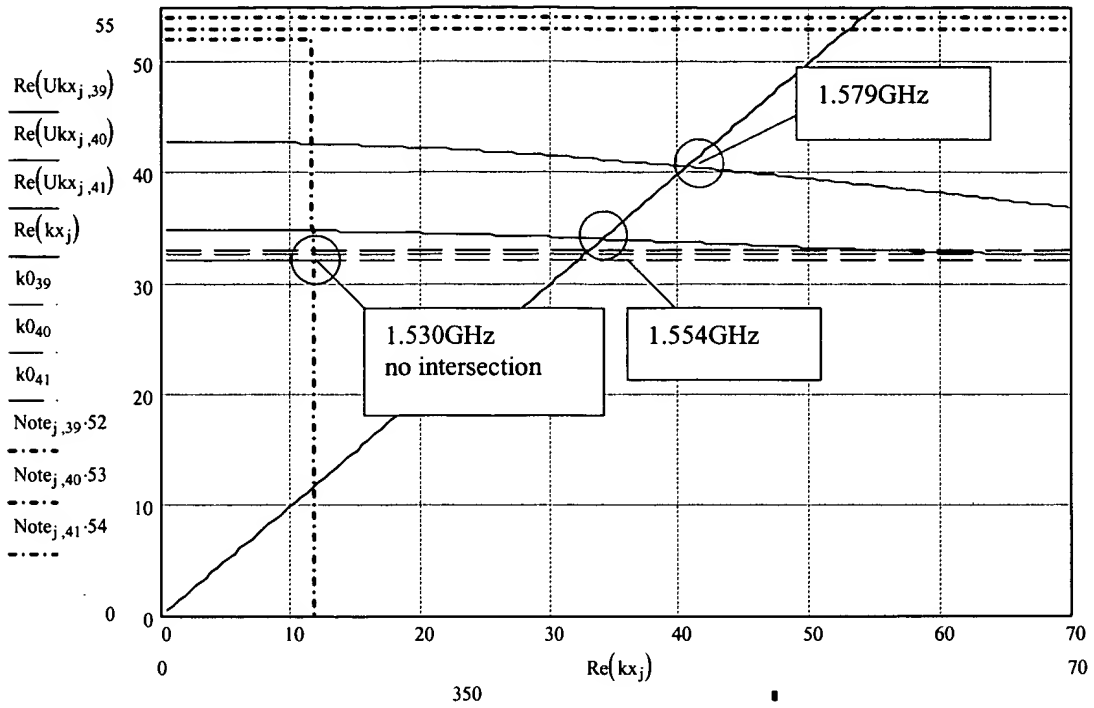

Figure 12. Plot of kx(TR) and kx versus kx. Intersection of the colored curves with the black line imply the existence of guided waves.

We can show that the problem is the varactors (particularly their inductance) by increasing the C_{square} to 0.73pF and dropping the parasitic inductance to 1nH. This is consistent with the assumption of an overlap two-sided FSS design and impossible to do with a single side (the gap would be 0.35mils). The result is Figure 13, where the resonance is at around 1.57GHz (-3° phase) but we do not get an intersection until 1.634 GHz (the –38.6° phase point). But even with low inductance, the artificial increase of capacitance without a drop in μ_z would still limit the surface wave suppression bandwidth. In Figure 14, I set the parasitic inductance and the varactor inductance to 0. Now the resonance is just below 1.6GHz (-8° point), and the intersection does not occur until 1.70 GHz which is the –55.3° point. We clearly buy some bandwidth back but we cannot get any closer than this to the –90° point.

Of course the problem is worst at the maximumvalue of the varactor, where even in the absence of any parasitic inductance, the TE waves appear as soon as the resonance is crossed. Figure 15 shows this for this case where the resonance is just below 0.913GHz (the –8° point).

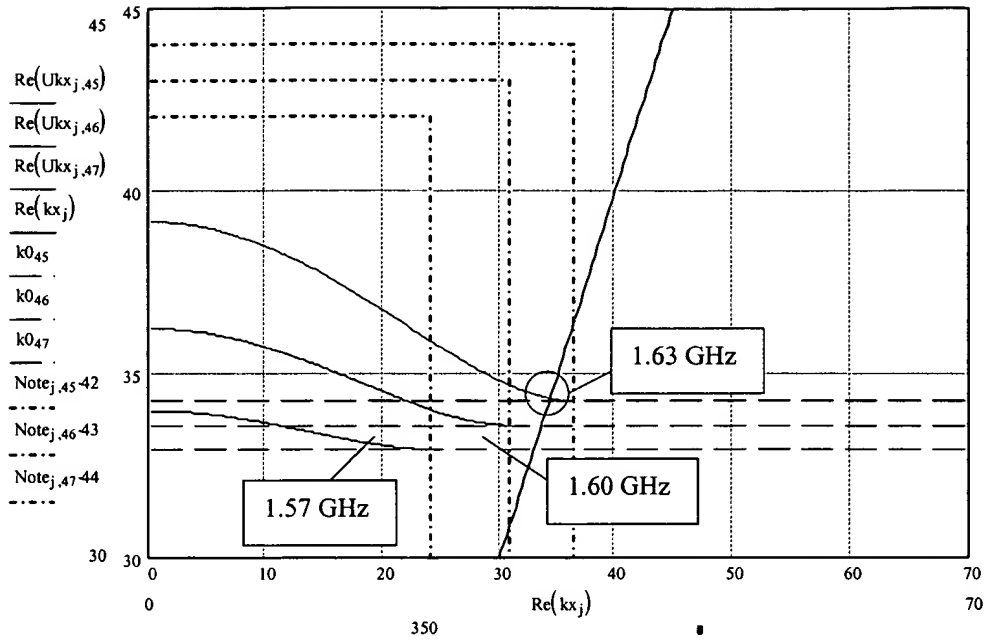

Figure 13. Same as Figure 12 but now the FSS has a geometric capacitance of 0.73pF and the parasitic inductance has been dropped to 1nH. TE waves do not start until 1.63 GHz.

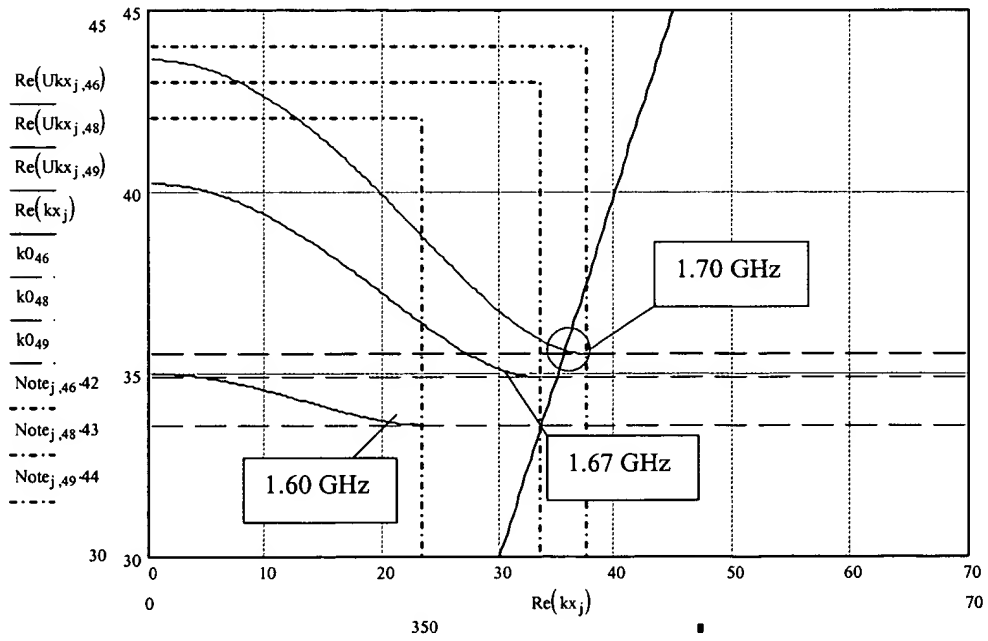

Figure 14. Same as Figure 13, except now all parasitic inductances (including Lp) have been set to zero. The TE modes do not appear until 1.7GHz, the -53° point.

The conclusion is that varactor tuned AMCs lose their ability to suppress TE surface waves (ie. the cutoff point is very near the 0° phase point). They only suppress TM surface waves through the negative ε_z effect of the bottom substrate's via array.

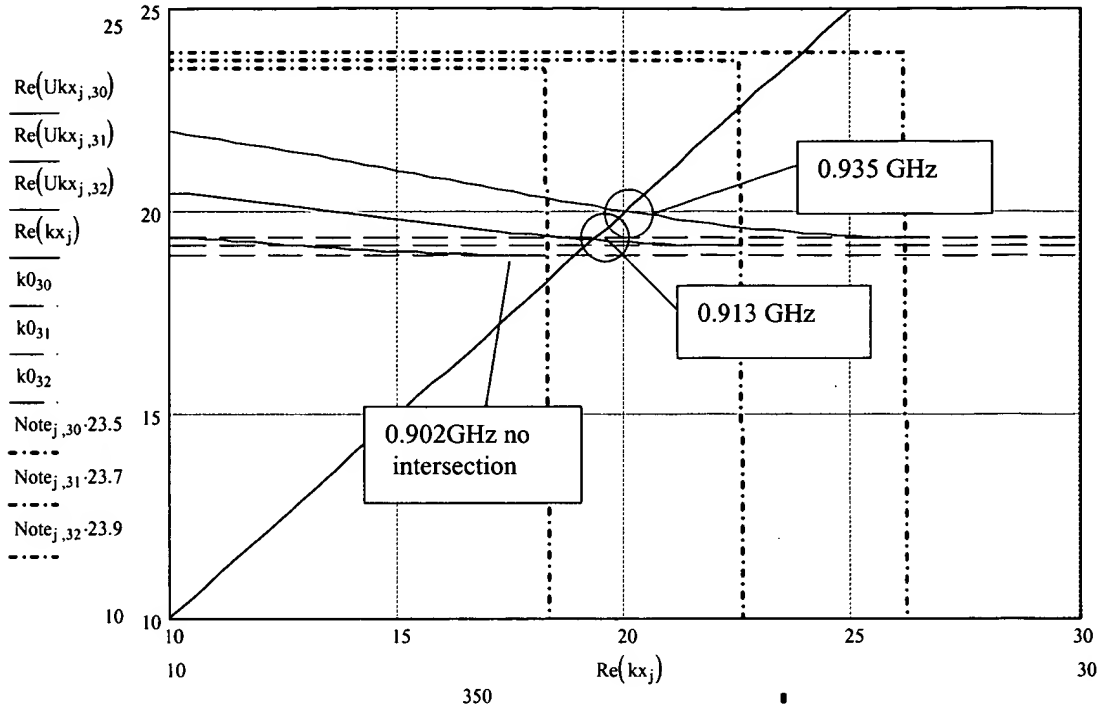

Figure 12. The best case of the 3x3 AMC with no parasitic inductance, a squares' capacitance of 0.73pF ad the varactor excess capacitance increased to 7pF. TE waves appear as soon as the resonance is crossed (0.902GHz).

Task 2.1 Identification of Desired Equivalent Media Properties, and Task 2.2 Fast Solver Development were completed during this reporting period. The salient details of this analysis were presented at the RECAP agents meeting briefing in mid-August. To summarize, we now have a detailed understanding of:

- How the physical layout of the Sievenpiper structure translates into effective media parameters
- How the transverse and axial effective media permittivities and permeabilities (of both the spacer and FSS layers) affect both reflection phase and surface wave characteristics of the structure.
- What materials/methods would be useful for increasing the AMC operational bandwidth

Task 2.3 Realizability of the Desired Effective Media: This task was started during this period. Its purpose is to use the tools developed in task 2.2 to analyze structures that may yield equivalent permittivities and permeabilities which were found desirable in task 2.1. For example, we have determined that low normal permeability in the FSS and spacer layers is desirable, in terms of pushing the TE band edge up in frequency as high as possible (near the +90° reflection phase point). This task will analyze structures, such as loops embedded in the spacer layer produce this effect.

Task 3.1 Narrow-Instantaneous-Band Reconfigurable Bandgap AMC Demonstration: The purpose of this task is to design, fabricate and test antenna elements over a reconfigurable AMC structure. The initial tuning mechanism to be realized consists of varactor diodes placed across the patches in a single layered capacitive FSS to obtain variable capacitance, hence a variable tuning state for the AMC. This is shown in figure 13 below. Note that only every 3rd patch will contain a varactor in the initial design to be realized (this is in order to reduce the complexity and cost of the design). Also, note that for clarity, the diagram below demonstrates the notion in only one polarization, but in practice we will realize the concept in both planes of the array.

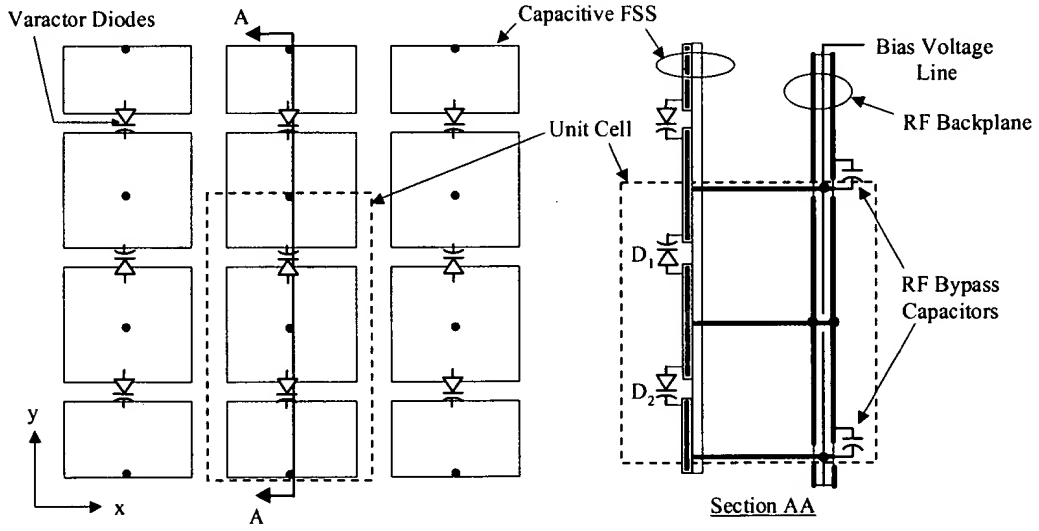

Figure 13. Concept Drawing of AMC Structure with Single-FSS-Layer Varactor-Tuning

The design specifics for the AMC structure realized is shown in figure 14 below. Initial modeling reported upon in the previous reporting period (and in section 1.2 above indicated an anticipated tuning range of between approximately 600 MHz and 2 GHz. Figure 15 shows the measured reflection phase while figure 16 shows the measured surface wave performance for 3 different bias states.

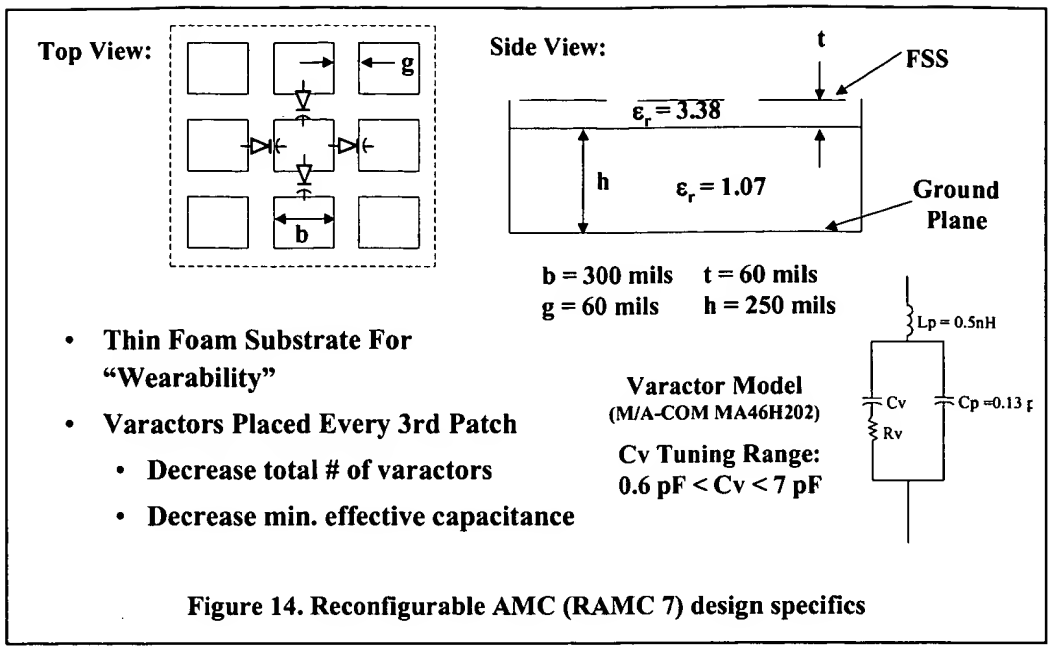

Figure 14. Reconfigurable AMC (RAMC 7) design specifics

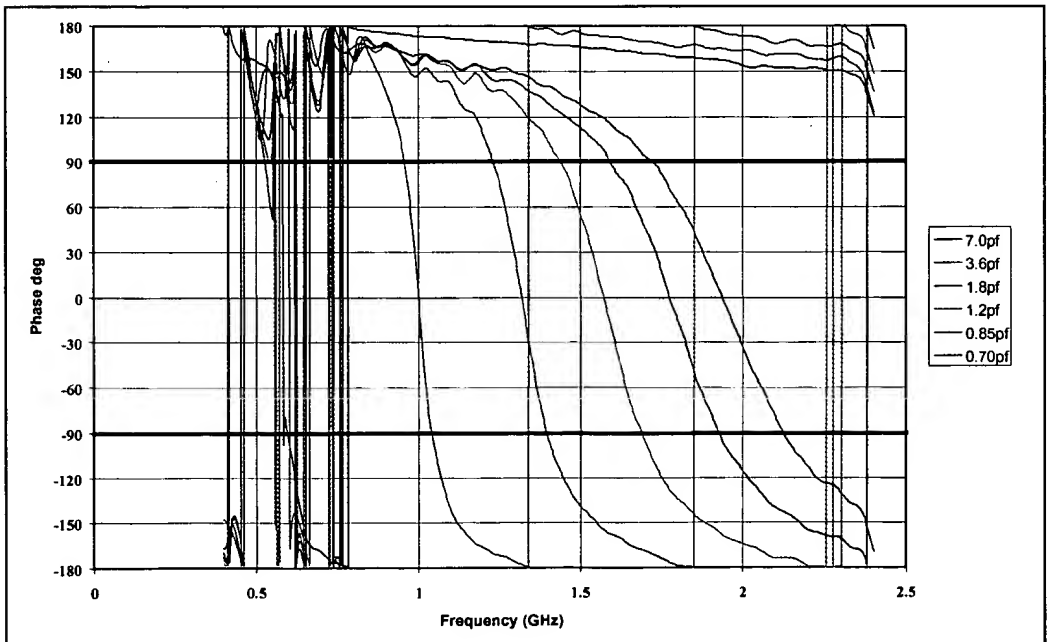

Figure 15. Measured Reflection Phase for Reconfigurable AMC in Various Bias States.

Varactors Biased at 16.6 V (Cv = 0.70 pF)

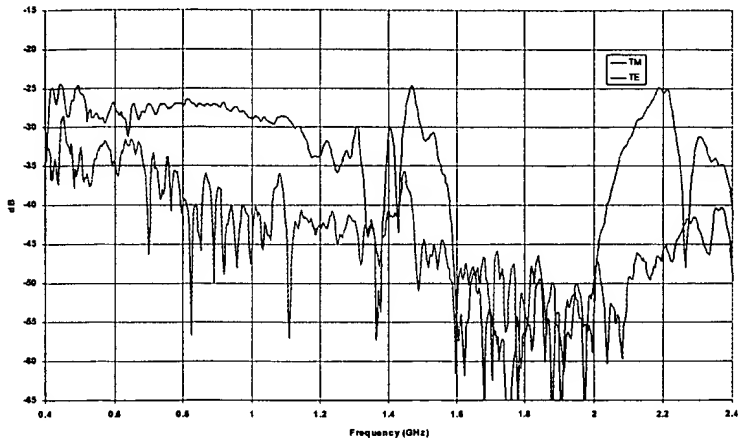

Varactors Biased at 6.7 V (Cv = 1.8 pF)

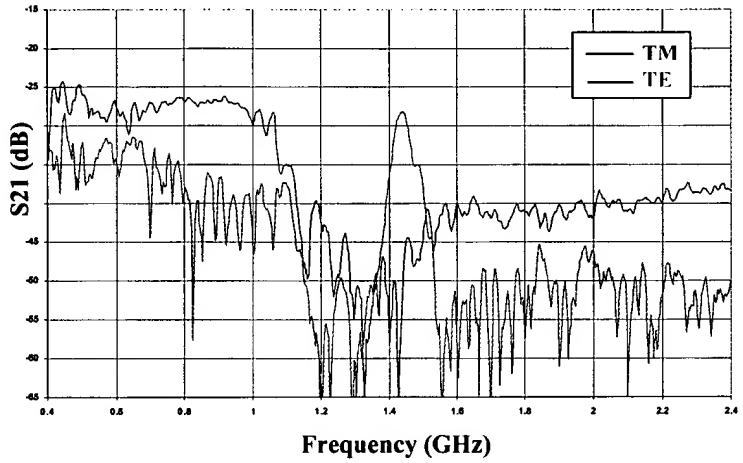

Varactors Biased at 0 V (Cv = 7.0 pF)

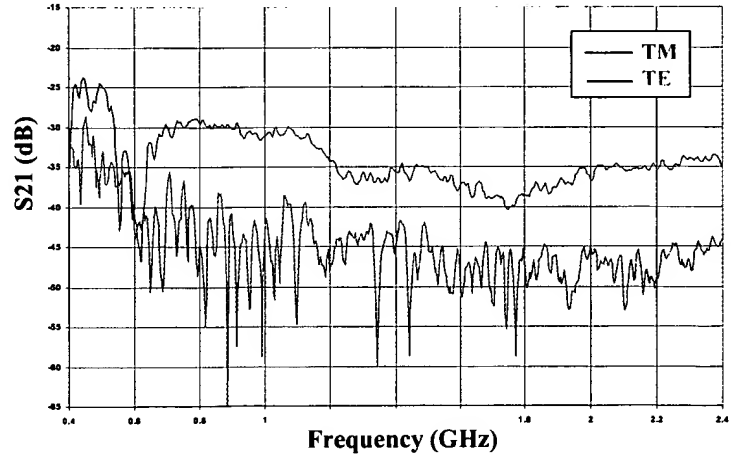

Figure 16. Measured Surface Wave Performance of Reconfigurable AMC in Three Different Bias States

The results are consistent with predictions and indicate that a varactor-tuned AMC surface is feasible. A high impedance and surface wave bandgap were demonstrated to tune over approximately a 3:1 tuning range (650 – 2100 MHz). Although it is difficult to define the exact band-edge of the TE surface waves (because these waves transform slowly from fast-leaky waves to slow, bound surface waves) the measurements do indicate that the TE band edge is lower in frequency than is optimal. This was predicted in the surface wave analysis (it falls out of the transcendental equations in the transverse resonance solution because the varactors increase transverse permittivity in the FSS layer without a proportional decrease in normal permeability). Alternative methods for tuning which do not have this limitation are being considered. The next step will be to fabricate and test broadband antennas over this surface. These results will be presented in the next report.

Task 4 Meetings and Reports:

The RECAP agents meeting took place on August 14th, 2000. In attendance representing the Atlantic/ASU team were Victor Sanchez, Bob Rawnick and Rudy Diaz. Some time was spent during early August to assemble technical information and prepare briefing slides.

5.0 Plans for the Next Month (October 2000)

In October we plan to continue our development of artificial magnetic materials with emphasis on barium-cobalt-hexaferrite development as well as the iron particle approach. We also plan to develop broadband frequency-independent antenna elements that will be used to assess the performance of the AMC as a broadband-groundplane. This will be done by measuring impedance and radiation patterns for the combined antenna-AMC structure. Additionally, some effort will be expended towards design and implementation of a second reconfigurable AMC substrate. This second design will employ a PIN diode mechanism in order to attempt to achieve greater tuning bandwidth and a TE band-edge which achieves the full Sievenpiper structure bandwidth.